Green synthesis, structural characterization, DFT, molecular docking and biological evaluation of some novel anti-cancer compounds

E Dhanalakshmi[1]*, P Rajesh[2], M Anbarasu[3], Arun Raaza[4] & M Prabhaharan[5]

[1]Department of Physics, Vel Tech Multi Tech Dr. Rangarajan Dr. Sakunthala Engineering College,
Avadi, Chennai-600 062, Tamil Nadu, India

[2]Department of Physics, School of Basic Sciences; [3]Department of Agronomy, School of Agriculture; & [4]Research and Development,
Vels Institute of Science, Technology & Advanced Studies, Pallavaram, Chennai-600 117, Tamil Nadu, India

[5]Department of Physics, Saveetha School of Engineering, Saveetha Institute of Medical and Technical Sciences (SIMATS),
Chennai-602 105, Tamil Nadu, India

The natural therapeutic properties of pharmacological compounds are used to treat numerous illnesses and various cancer therapies in traditional medicine. In this context, the herbal leaves of *Hybanthus enneaspermus, Aegle marmelos* and the flowers of *Calotropis gigantea* were examined by gas chromatography-mass spectrometry (GC-MS) analysis. The results exposed *Hybanthus enneaspermus, Aegle marmelos* leaves and *Calotropis gigantea* flowers contain many anti-bacterial, anti-inflammatory and anti-cancer (Prostate cancer, Renal cell carcinoma, Leukemia, colon, skin, colon, liver, prostate, and apoptosis) activity. Thus, there is a higher amount of strong cancer therapy properties present within *Calotropis gigantean* extract than leaves of *Hybanthus enneaspermus, Aegle marmelos* in natural medicine. The compounds revealed the potential to cure cancer treatment conformed through molecular docking by using cancer receptors for predicted binding affinity. The crystal structure of 8D59 (METTL1) and ligands were obtained from the Protein Database and PubChem server, ChemDraw Ultra 12.0 software. Among the compounds exhibit the best binding affinity of -8.83 kcal/mol concerning 3', 8, 8'-Trimethoxy-3-piperidyl-2, 2'-binaphthalene-1, 1', 4, 4'-tetrone. These components express ADME properties and also satisfy Lipinski's rules for oral bioavailability. The optimized geometry structure of the bond angle and bond length of seventeen compounds has been obtained by DFT/B3LYP/6-311++G(d, p) set in Gaussian 09W software.

Keywords: ADMET, DFT, Docking study, Drug-likeness, GC-MS

Cancer appears as the second most prevalent cause of death and sickness in humans. An estimated 20 million different cases of cancer and 10 million cancer-related deaths occurred worldwide reported by the World Health Organization. The natural therapeutic properties of bioactive components to the development of multi-treatment techniques for use in cancer treatment[1]. The herbs play a vital role in therapeutic properties and are used effectively to treat the diseases of humans. Usually, the bioactive compounds synthesized from medicinal plants such as alkaloids, polyphenols, glycosides, and terpenes have been used to treat therapeutic and pharmacological action. Moreover, 80% of phytochemicals isolated, characterized and identified as drugs from herbal plants used in modern medicine have a favourable correlation between their historic uses and newer therapeutic applications[2]. Some of the herbs are commonly used to create a novelty in the pharmaceutical sector, cost-effectively in the herbal remedies for the treatment of different human disorders[3]. Wisely, the medicinal plants of blue spade (*Hybanthus enneaspermus*), beal (*Aegle marmelos*) both herbs leave and giant milkweed (*Calotropis gigantea*) flowers have hadenormous medicinal properties anti-inflammation, anti-microbial, anti-tumour and are highly used in herb, their family and scientific name as given in (Table 1). A larger percentage of different areas such as Ayurveda, Siddha, and clinical prevention were demonstrated by the comprehensive method for antioxidant, antidiabetic and antiurolithiatic properties of silver nanoparticles synthesized from leaves of *Hybanthus enneaspermus*[4]. The beal (*Aegle marmelos)* is also a botanical entity and pharmaceutical medicine made highly from the leaf which is used for a wide range of illnesses to cure fever, diabetes, heart issues, diarrhea, asthma, and urinary tract problems. *Aegle marmelos* possess cancer activity such as leukemia, melanoma

*Correspondence:
E-mail: jdkrishii2015@gmail.com

Common Name	Scientific Name	Family	Common uses
Blue Spade Flower / Ratanpurus / Orithalthamarai	*Hybanthus enneaspermus*	*Violaceae*	Tonic for pregnant women, treatment of diarrhea, urinary infections, leucorrhoea, dysuria, inflammation, cancer – activity.
Bael / Golden apple / Vilvam	*Aegle marmelos*	*Rutaceae*	Treating fever, nausea, vomiting, swellings, dysentery, dyspepsia, seminal weakness, and intermittent fever, urinary problems, and cancer activity.
Crown flower / Giant milkweed / Erukkam poo	*Calotropis gigantea*	*Apocynaceae*	Treat fevers, Neurological disorders, cancer activity, and antidote for snake bite, vomiting, and diarrhea.

Table 1 — The common name, scientific name, family and uses of *Hybanthus enneaspermus, Aegle marmelos* and *Calotropis gigantea*

and breast cancer cell lines[5]. The traditional flower of *Calotropis gigantea* usually includes important drug properties in various medicinal fields such as numerous long-term inflammatory conditions that can be using herbal treatment and antioxidants effectively. The qualitative and quantitatively various bio components like alkaloids, terpenoids, phenols and flavonoids. The natural biological mechanism of anticancer impact, lead bioactive substances employing molecular docking method, respectively[6, 7]. To the best of our understanding, the above literature evaluation has not yet been done any identified and compared strong potential cancer efficiency in the medicinal extract of *Hybanthus enneaspermus, Aegle marmelos* leaves and flower of *Calotropis gigantea.* In this study, the gas chromatography-mass spectrometry (GC-MS) analysis of carbinol extract from leaves and flowers to identify the multiple bioactivity compounds successively. Furthermore, the work to follow the computational analysis of density functional theory(DFT) using B3LYP/6-311++G(d, p) method interpreted by identified cancer activity compounds from leaves extract of *Hybanthus enneaspermus, Aegle marmelos* leaves and flowers of *Calotropis gigantea* for structure conformation. Thus, the biological evaluation of molecular docking analysis for ligand-protein interaction, drug-likeness, and absorption, distribution, metabolism, excretion (ADME) properties of seventeen phytochemicals.

Materials and Methods

Materials collection and sample preparation of *Hybanthus enneaspermus, Aegle marmelos* and *Calotropis gigantea*

The *Hybanthus enneaspermus, Aegle marmelos* leaves *and Calotropis gigantea* flowers samples were collected from Villages, Thiruvallur District, Tamil Nadu, India. The leaves and flowers were collected each 2 kilogram was washed with normal water and allowed to shade dry at normal room temperature for up to 2 weeks and then crushed into a fine powder used by an electrical mixer. The powder dipped in carbinol 95.5 % at a 2:1 ratio which was left
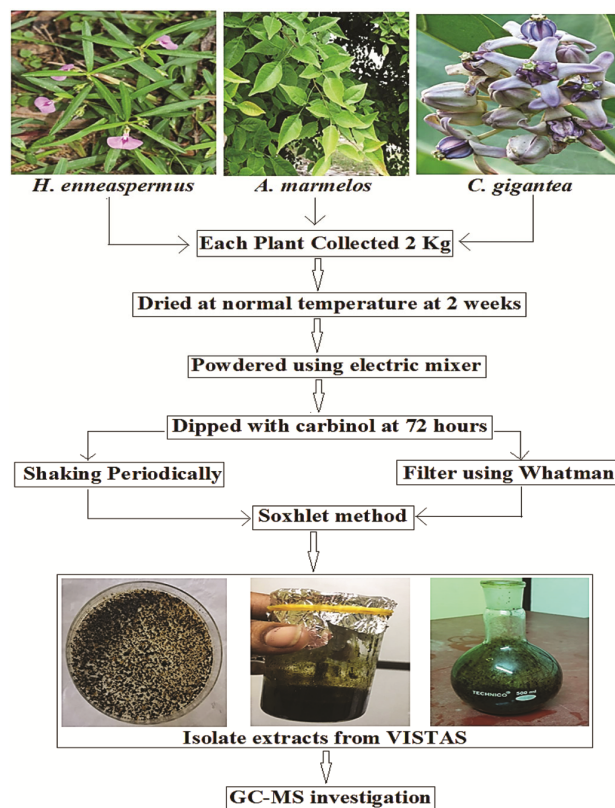
Scheme. 1 — Extraction of phytochemicals from *Hybanthus enneaspermus, Aegle marmelos* and *Calotropis gigantea*

at room temperature for 72 h and rotated periodically. The soxhlet method at 40°C to separate crude is shown in (Scheme 1). For later usage, all of the crudes had been stored fresh in an airtight container, respectively.

Experimental details

The GC-MS is a potent analytical method to detect various chemicals in the sample and to find extensive use in a variety of applications. It is great perception, effectiveness and capacity to evaluate complicated mixtures in a sample. The natural phytochemical compounds were found in extracts of *Hybanthus enneaspermus, Aegle marmelos* leaves and *Calotropis gigantea* flowers identified by GC-MS (Toshvin

Analytical, Shimadzu-QP2010 with stratum water analyzer) The GC-MS instrument has been maintained temperature from 4- 450°C and the carrier gas control has advanced flow controller. The detectors using FID, BID, TCD, ECD and MS scan range were set at 45 to 450 MHz and samples had a total working time of 55 minutes. The phytochemical components' fragment patterns of their mass spectrum have been compared with the spectrometer database through the NIST mass spectral library. The percentage of those compounds identified in the chromatography through relative peak, molecular weight and molecular formula, respectively.

Ligand -protein selection and preparation

The METTL1 complex was found to prevent the development resulting in numerous cancers, which include lung, liver, colon, bladder cancer and neck, head, also tumours. The METTL1 can be utilized as diagnostics or potential targets for treatment, opening up fresh possibilities for early cancer identification[8]. The protein 8D59 belongs to the crystal structure of human METTL1 in complex with SAM under the classification of transferase and has been examined through RCSB PDB server as displayed in (Fig. 1) and downloaded PDB format. The optimized three-dimensional structures of the compounds have been interpreted by ChemDraw Ultra software and converted into PDB basic format file. Completely, the seventeen bio-components identified from extracts of *Hybanthus enneaspermus, Aegle marmelos* leaves and *Calotropis gigantea* flowers have been chosen for this investigation, respectively.

Molecular docking and drug-likeness protocol

Molecular docking is frequently determining the impact on drug development for therapeutic agents. The computational docking process is used to estimate the bonding structure and the free energies involved in the binding of tiny molecules (ligand) to macromolecular receptors, which provides more knowledge into the inhibitory process and interaction modes[20]. The ligand was a dock with protein 8D59 (METTL1) into active location have been performed by AutoDock tool using Lamarckian genetic algorithm, which explores the accuracy of binding affinity of ligand and target receptor[9]. The AutoGrid including the grid box dimension within X, Y and Z direction was estimated and limarkian GA process revealed the maximum 10 conformers among ligand - receptor complexes were created for seventeen phytocompounds and the resulting docking score was correlated with each other. Furthermore, the
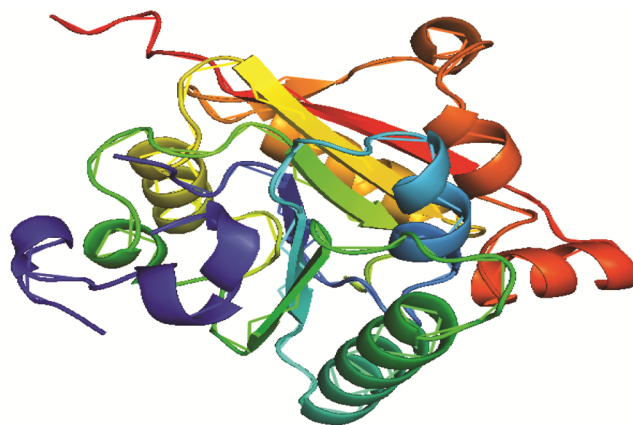

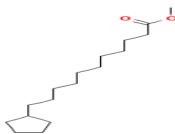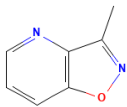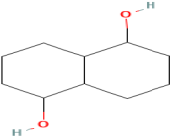Fig. 1 — Illustrate the protein 8D59 (METTL1)
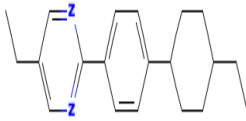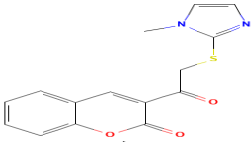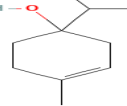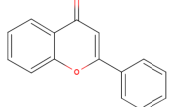
visualization tools for supporting in that order, Pymol, MGL tool and Phython software. The selected compounds were evaluated for drug-likeness based on five Lipinski rule have been estimated by using pkCSM - Biosig Lab online server[10]. The drug-likeness express their logP, molecular weight, hydrogen bond donors and acceptors, surface area was applied to identify potential compounds for use as oral medication in pharmacokinetic properties. The DFT/B3LYP/6-311++G(d, p) bases set was used to estimate the three-dimensional optimized structure of seventeen bio-compounds for structure conformation and molecular behaviour for biological prediction[11].
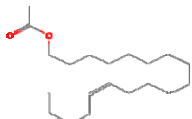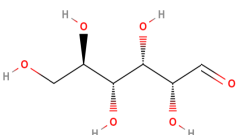
Results and Discussion

GC-MS analysis by extract of *Hybanthus enneaspermus* leaves

The GC-MS evaluation is one of the most often used techniques for separating organic substances from extracts of medicinal plants. The GC-MS analysis of carbinol extracts of various leaves namely *Hybanthus enneaspermus, Aegle marmelos* and flowers of *Calotropis gigantea* revealed major multiple phytochemical and bio-activity compounds. The result of GC-MS spectra identified the compounds based on molecular structure, molecular formula, molecular weight and retention time which are compared with the NIST database[12]. In the current research, the GC-MS result recorded twelve majorpharmacological bio-components from carbinol extract of *Hybanthus enneaspermus* as listed in (Table 2). From the twelve components only six phytochemicals present anti-tumor efficiency namely 3-Methylisoxazolo [4, 5-b]pyridine exhibits antiviral, anticancer activity, 1, 5-naphthalenediol, decahydro- has possesses anti-cancer efficiency, Pyrimidine, 5-ethyl-2-[4-(4-ethylcyclohexyl)phenyl] were exhibit antiviral,

Table 2 — Identified the phytochemicals from extract of *Hybanthus enneaspermus* leaves

S.No	Retention time (min)	Area %	Name of the Compound	Molecular Formula	Molecular Weight	Molecular Structure	Biological Activity & References
1	11.97	55.3	Cyclopentaneundecanoic acid, methyl ester	$C_{10}H_{18}O$	154.24		Antibacterial Activity
2	13.10	8.0	3-Methylisoxazolo [4, 5-b]pyridine	$C_7H_6N_2O$	134.00		Anti-inflammatory anti-cancer[13]
3	14.90	10.6	1, 5-naphthalenediol, decahydro-	$C_{10}H_{18}O_2$	170.25		Anti-cancer activity[14]
4	16.63	65.6	Hexadecanamide	$C_{16}H_{33}NO$	255.44		Inflammatory activity
5	19.07	14.9	Pyrimidine, 5-ethyl-2-[4-(4-ethylcyclohexyl) phenyl]	$C_{20}H_{26}N_2$	294.434		Anti-viral, anti-tumor, anti-cancer[15]
6	21.40	13.2	Coumarine, 3-[2-(1-methyl-2-imidazolylthio)-1-oxoethyl]	$C_{15}H_{12}N_2O_3S$	300.00		Prostate cancer, Renal cell carcinoma[16]
7	11.97	3.3	3-Cyclohexen-1-ol, 4-methyl-1-(1-methyllethyl)-	$C_{10}H_{18}O$	154.24		antimicrobial activities
8	16.03	58.6	Flavone	$C_{15}H_{10}O_2$	222.24		anti-cancer activity[17]
9	18.38	49.4	Octadec-9-enoic acid	$C_{18}H_{34}O_2$	282.5		anti-inflammatory and anti-cancer[18]
10	20.30	13.2	Z-13-Octadecen-1-yl acetate	$C_{20}H_{38}O_2$	310.5		Improve the stand ard sex pheromones
11	23.62	6.7	Hexadecyl 3-methylbutanoate	$C_{21}H_{42}O_2$	326.0		Anti-microbial effect
12	14.20	6.5	Glucose	$C_6H_{12}O_6$	180.16		Metabolization in cancer cell[19]
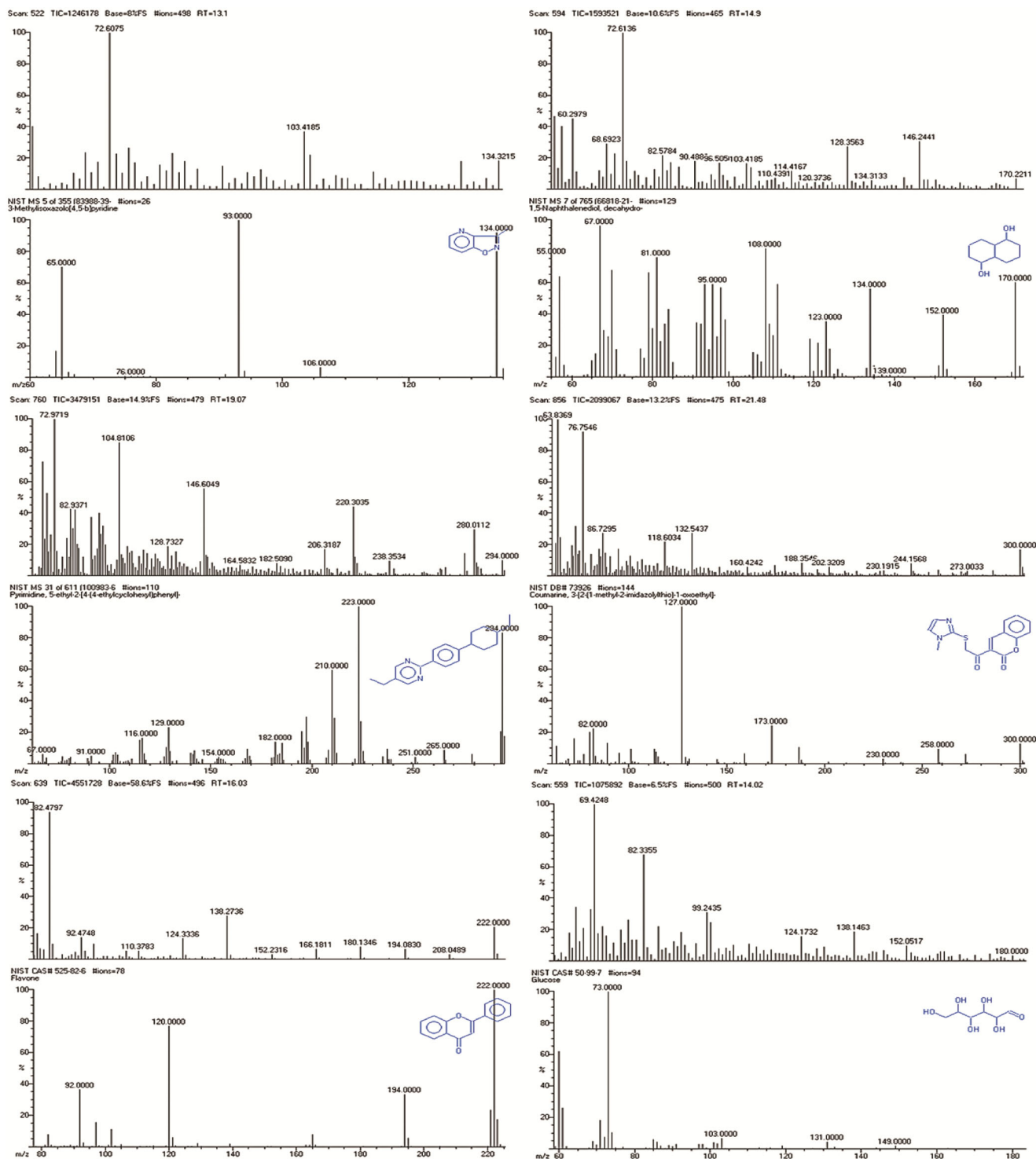
Fig. 2 — The GC-MS result of phytocompounds identified from *Hybanthus enneaspermus*

antitumor effected, Coumarine, 3-[2-(1-methyl-2-imidazolylthio)-1-oxoethyl] compound displayed prostate cancer, renal cell carcinoma and leukemia. Flavone and Glucose also exhibited anti-therapeutic effects, which compounds identified through NIST library based on molecular formula ($C_7H_6N_2O$, $C_{10}H_{18}O_2$, $C_{20}H_{26}N_2$, $C_{15}H_{12}N_2O_3S$, $C_{15}H_{10}O_2$ and $C_6H_{12}O_6$), molecular weight (134.00, 170.25, 294.43, 300.00, 222.24 and 180.16 g/mol) retention time (13.10, 14.90, 19.07, 21.40, 16.03 and 14.20 min) and area (8.0, 10.6, 14.9, 21.40, 16.03 and 14.20 %) GC-MS results as shown in (Fig. 2), respectively.

GC-MS analysis by extract of *Aegle marmelos* leaves

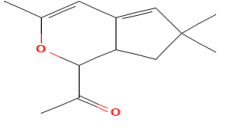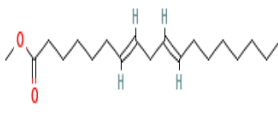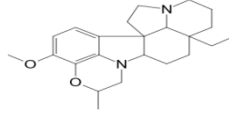The GC-MS investigated carbinol extract of *Aegle marmelos* shows eight bio-activity components and their two dimensional structures, biological activity as shown in (Table 3). Among the eight compounds, the anti-cancer activity occupied only one pharmacological molecule 1-(3, 6, 6-Trimethyl-1, 6, 7, 7a-tetrahydro cyclopenta [c]pyran-1-yl) ethanonen shows well anti-tumour activity. The GC-MS results recorded phytochemical confirmed through molecular formula ($C_{13}H_{18}O_2$), molecular weight (206.28 g/mol) and retention

time (17.38 min) and area (78.1%) as shown in (Fig. 3) that are found in the NIST database, respectively.

GC-MS analysis by extract of *Calotropis gigantea* flower

The GC-MS evaluation of carbinol extract of *Calotropis gigantea* flowers recorded twenty-four major compounds and their structures, molecular weight g/mol, molecular formula, retention time (min) and area %as listed in (Table 4). From that ten compounds present high anti-malignant tumour activities given below 1-cyclohexanol,

Table 3 — Identified phytochemicals from extract of *Aegle marmelos* leaves
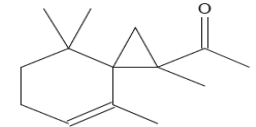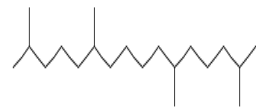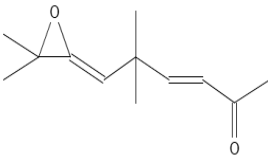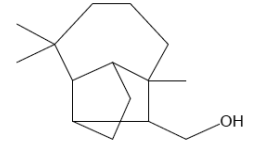
S. No	Retention time (min)	Area %	Name of the Compound	Molecular Formula	Molecular Weight	Molecular Structure	Biological Activity & References
1	16.18	17.9	Methyl Z-11-tetradecenoate	$C_{15}H_{28}O_2$	240.38		Anti-microbial resistance
2	17.38	78.1	1-(3, 6, 6-Trimethyl-1, 6, 7, 7a-tetrahydrocyclopenta[c]pyran-1-yl)ethanone	$C_{13}H_{18}O_2$	206.28		Anti-cancer activity[20]
3	18.47	100	Hexadecanoic acid, methyl ester	$C_{17}H_{34}O_2$	270.45		Anti-microbial activity[21]
4	20.40	71.5	Dodecanoic acid, methyl ester	$C_{13}H_{26}O_2$	214.19		Anti-microbial estimated
5	20.65	100	Heptadecanoic acid, 16-methyl-, methyl ester	$C_{19}H_{38}O_2$	298.50		Metabolites, Microbiota profiles[22]
6	21.40	23	7, 10-Octadecadienoic acid, methyl ester	$C_{19}H_{34}O_2$	294.5		Anti-inflammatory[23]
7	23.03	25.4	Octadecanoic acid, 17-oxo-, methyl ester	$C_{19}H_{36}O_3$	312.50		Anti-inflammatory properties[23]
8	24.75	16.2	4, 25-Secoobscurinervan, 21-deoxy-16-methoxy-23-methyl-	$C_{23}H_{32}N_2O_2$	368.00		No activity

1-(3,6,6-Trimethyl-1,6,7,7a-tetrahydrocyclopenta[c]pyran-1-yl)ethanone
C13H18O2; MF: 839; RMF: 847; Prob 78.1%; Lib: mainlib; ID: 156629.
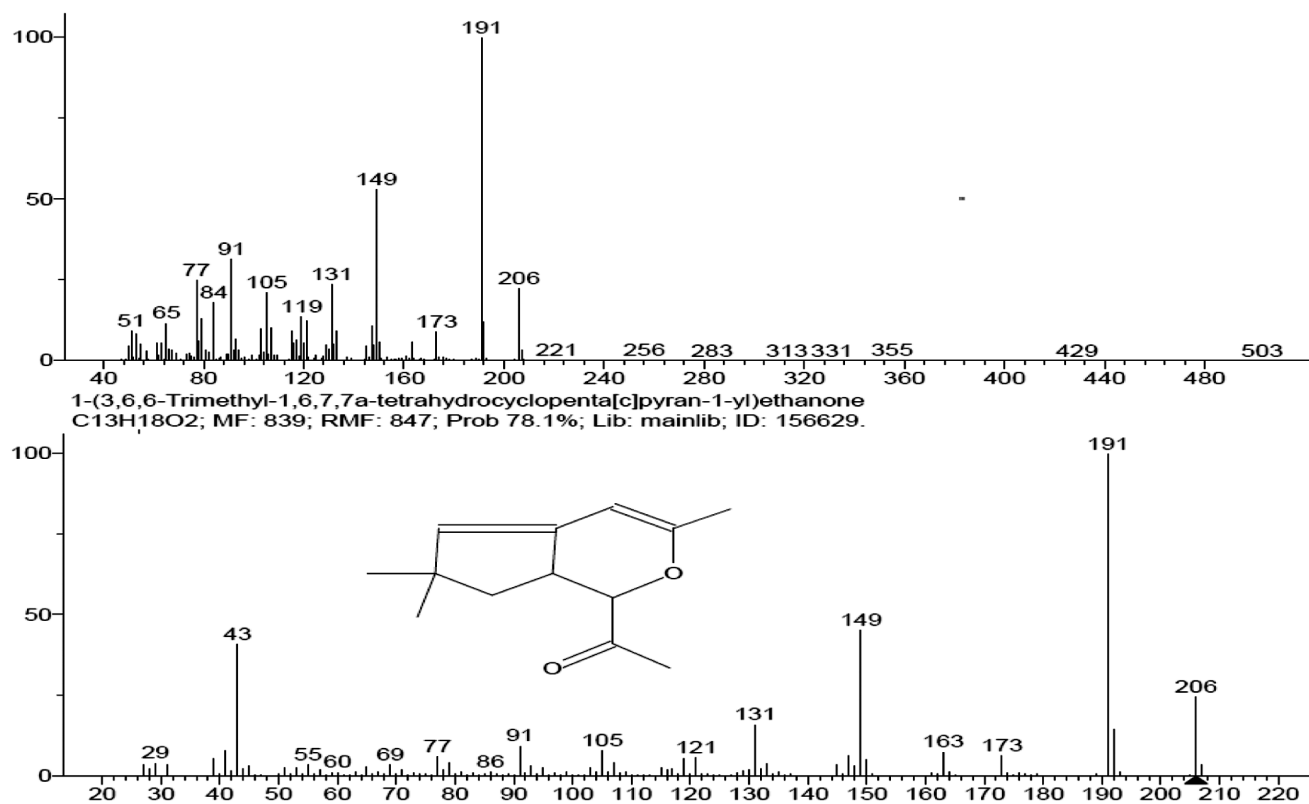
Fig. 3 — The GC-MS result of phytocompounds identified from *Aegle marmelos*

Table 4 — Identified the phytochemicals from extract of *Calotropis gigantean* flowers

S. No	Retention time (min)	Area %	Name of the Compound	Molecular Formula	Molecular Weight	Molecular Structure	Biological Activity & References
1	3.69	1.06	2, 5-Norbornadiene	C_7H_8	92.06		Nematicidal activity[24]
2	3.845	52.2	Benzene, (2, 4-dimethylpentyl)-	$C_{13}H_{20}$	176.15		anti-oxidant effects[25]
3	42.22	13.4	1-Cyclohexanol, 2-(3-methyl-1, 3-butadienyl)-1, 3, 3-trimethyl-	$C_{14}H_{24}O$	208.18		Colon cancer[26]
4	42.29	21.8	2, 5, 5, 6, 8a-Pentamethyl-trans-4a, 5, 6, 7, 8, 8a-hexahydro-gamma-chromene	$C_{14}H_{24}O$	208.18		Prostate Cancer[27]
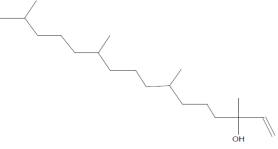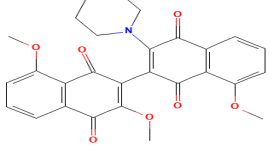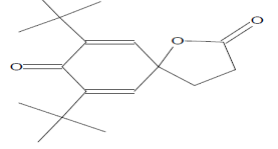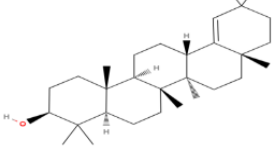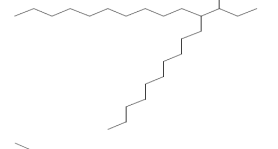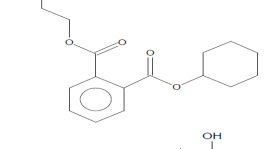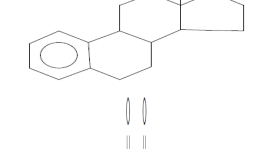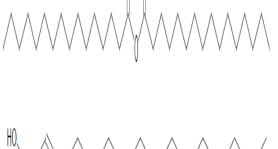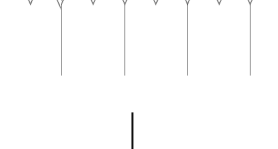
(*Contd.*)

Table 4 — Identified the phytochemicals from extract of *Calotropis gigantean* flowers (*Contd.*)

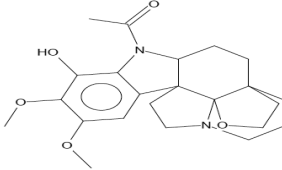| S. No	Retention time (min)	Area %	Name of the Compound	Molecular Formula	Molecular Weight	Molecular Structure	Biological Activity & References
5	42.66	21.0	Geranylisovalerate	$C_{15}H_{26}O_2$	238.19		Anti-microbial activity
6	42.71	27.6	Spiro[2.5]oct-4-ene, 1-acetyl-1, 4, 8, 8-tetramethyl-	$C_{14}H_{22}O$	206.16		Pharmacological analysis
7	43.13	7.72	Hexadecane, 2, 6, 11, 15-tetramethyl-	$C_{20}H_{42}$	282.32		Antibacterial activity
8	44.02	19.2	6-(3, 3-Dimethyl-oxiran-2-ylidene)-5, 5-dimethyl-hex-3-en-2-one	$C_{12}H_{18}O_2$	194.13		Anti-cancer and ADME properties[28]
9	44.10	13.2	1, 4-Methanoazulene-9-methanol, decahydro-4, 8, 8-trimethyl-, [1S-(1α, 3aβ, 4α, 8aβ, 9R*)]-	$C_{15}H_{26}O$	222.19		Liver cancer[29]
10	44.56	8.36	Eicosane, 2-methyl-	$C_{21}H_{44}$	296.34		Anti-fungal
11	44.60	11.9	Aspidospermidin-17-ol, 1-acetyl-19, 21-epoxy-15, 16-dimethoxy-	$C_{23}H_{30}N_2O_5$	414.21		Anti-tumour and anti-malarial[30]
12	44.96	6.22	Heptadecane, 2, 6, 10, 15-tetramethyl-	$C_{21}H_{44}$	296.34		Anti-inflammatory effect
13	45.36	4.33	1-Decanol, 2-hexyl-	$C_{16}H_{34}O$	242.26		Anti-bacterial activity
14	45.85	11.3	Cyclohexanone, 2, 3-dimethyl-2-(3-oxobutyl)-	$C_{12}H_{20}O_2$	196.14		Colon cancer[26]

(*Contd.*)

Table 4 — Identified the phytochemicals from extract of *Calotropis gigantean* flowers (*Contd.*)
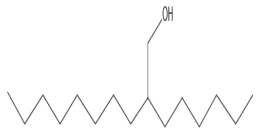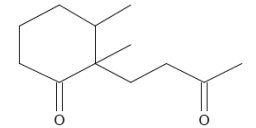
S. No	Retention time (min)	Area %	Name of the Compound	Molecular Formula	Molecular Weight	Molecular Structure	Biological Activity & References
15	46.38	1.72	Isophytol	$C_{20}H_{40}O$	296.30		Anti-microbial activity
16	46.43	6.91	3', 8, 8'-Trimethoxy-3-piperidyl-2, 2'-binaphthalene-1, 1', 4, 4'-tetrone	$C_{28}H_{25}NO_7$	487.16		Apoptosis cancer[31]
17	47.14	91.5	7, 9-Di-tert-butyl-1-oxaspiro(4, 5)deca-6, 9-diene-2, 8-dione	$C_{17}H_{24}O_3$	276.17		Anti-cancer Properties[32]
18	47.21	0.19	Germanicol	$C_{30}H_{50}O$	426.38		Colon cancer[33]
19	47.62	2.75	Heneicosane, 11-(1-ethylpropyl)-	$C_{26}H_{54}$	366.42		Anti-microbial activity
20	47.86	2.98	1, 2-Benzenedicarboxylic acid, butyl cyclohexyl ester	$C_{18}H_{24}O_4$	304.16		Cytotoxicity against cancer cell line[34]
21	48.00	34.0	Estra-1, 3, 5(10)-trien-17β-ol	$C_{18}H_{24}O$	256.18		Liver cancer[35]
22	48.24	8.70	Palmitic anhydride	$C_{32}H_{62}O_3$	494.46		Antimicrobial and antioxidant properties
23	50.79	78.5	Phytol	$C_{20}H_{40}O$	296.30		cytotoxic activity
24	3.64	17.6	Toluene	C_7H_8	92.06		Anti-bacterial activity

2-(3-methyl-1, 3-butadienyl)-1, 3, 3-trimethyl-derivatives cause HCT116 colon tumour cells to undergo apoptosis and block AChE activity. 2, 5, 5, 6, 8a-pentamethyl-trans-4a, 5, 6, 7, 8, 8a-hexahydro-gamma-chromene explore effectiveness in males suffering from castrate-resistant prostate carcinoma. 6-(3, 3-dimethyl-oxiran-2-ylidene)-5, 5-dimethyl-hex-3-en-2-one shows the anti-cancer and ADME properties. 1, 4-meth-anoazulene-9-methanol, decahydro-4, 8, 8-trimethyl-, [1S-(1α, 3aβ, 4α, 8aβ, 9R*)]- asses effective colon-cancer activity. Cyclohexanone, 2, 3-dimethyl-2-(3-oxobutyl)- has been determined high level of anti-cancer effectiveness. 3', 8, 8'-trimethoxy-3-piperidyl-2, 2'-binaphthalene-1, 1', 4, 4'-tetrone, 7, 9-di-tert-butyl-1-oxaspiro (4, 5)deca-6, 9-diene-2, 8-dione demonstrated that in both KYSE-450 and Eca-109 liver esophageal

cancer cells. Germanicol has been demonstrating specific antiproliferative efficiency against two lines of human colon tumor cells. 1, 2-benzenedicarboxylic acid, butyl cyclohexyl ester estimate cytotoxicity against cancer cell line. Furthermore, estra-1, 3, 5(10)-trien-17β-ol can explore liver, prostate and breast cancer, which compounds identified through NIST library based on molecular formula ($C_{14}H_{24}O$, $C_{14}H_{24}O$, $C_{12}H_{18}O_2$, $C_{15}H_{26}O$, $C_{12}H_{20}O_2$, $C_{28}H_{25}NO_7$, $C_{17}H_{24}O_3$, $C_{30}H_{50}O$, $C_{18}H_{24}O_4$, $C_{18}H_{24}O$), molecular weight (208.18, 208.18, 194.13, 222.19, 196.14, 487.16, 276.17, 426.38, 304.16 and 256.18) retention time (42.22, 42.29, 44.02, 44.10, 45.85, 46.43, 47.14, 47.21, 47.86 and 48.00 min) and area (13.4, 21.8, 19.2, 13.2, 11.3, 6.91, 91.5, 0.19, 2.98 and 34.0%), which GC-MS results as illustrated in (Fig. 4), respectively.

Fig. 4 — The GC-MS result of phytocompounds identified from *Calotropis gigantean* (*Contd.*)

Cyclohexanone, 2,3-dimethyl-2-(3-oxobutyl)-
C12H20O2; MF: 690; RMF: 732; Prob 11.3%; CAS: 98361-31-0; Lib: mainlib; ID: 6427.

3',8,8'-Trimethoxy-3-piperidyl-2,2'-binaphthalene-1,1',4,4'-tetrone
C28H25NO7; MF: 607; RMF: 646; Prob 6.91%; CAS: 127611-84-1; Lib: mainlib; ID: 121431.

7,9-Di-tert-butyl-1-oxaspiro(4,5)deca-6,9-diene-2,8-dione
C17H24O3; MF: 847; RMF: 870; Prob 91.5%; CAS: 82304-66-3; Lib: mainlib; ID: 25093.

Germanicol
C30H50O; MF: 567; RMF: 585; Prob 0.19%; CAS: 465-02-1; Lib: mainlib; ID: 164783.

1,2-Benzenedicarboxylic acid, butyl cyclohexyl ester
C18H24O4; MF: 899; RMF: 923; Prob 2.98%; CAS: 84-64-0; Lib: mainlib; ID: 122677.

Estra-1,3,5(10)-trien-17β-ol
C18H24O; MF: 711; RMF: 730; Prob 34.0%; CAS: 2529-64-8; Lib: mainlib; ID: 7345.

Fig. 4 — The GC-MS result of phytocompounds identified from *Calotropis gigantean*

PROTEIN : 8D59 (METT1)

Fig. 5 — Ligand -protein interactions of anti-cancer compounds identified from *Hybanthus enneaspermus* within the active site of METT1 (1a)3-methylisoxazolo [4, 5-b] pyridine;(1b) 1, 5-naphthalenediol, decahydro-;(1c) pyrimidine, 5-ethyl-2-[4-(4-ethylcyclohexyl) phenyl];(1d)coumarine, 3-[2-(1-methyl-2-imidazolylthio)-1-oxoethyl]; (1e) flavone; and (1f)glucose

Molecular docking and drug-likeness analysis

The tRNAs are modified by m7G, which is catalyzed by the RNAmethyltransfer receptor METT1. In this section researchers demonstrate that METT1 is frequently enhanced and amplified in cancerand inhibits oncogenicity. Therefore, the METT1 mediated tRNA alteration is a potential target for anti-cancer therapy, because it stimulates tumor progression by altering the mRNA "translatome" to the development of a growth-promoting receptor. The section of chromosome 12 (12q 13-14) that often increases in target tumor is linked to METTL1 and major inhibition of primary murine AML cells[36]. The *Hybanthus enneaspermus, Aegle marmelos* leaves & *Calotropis gigantea* flowers expressed seventeen anti-cancer compounds investigated by molecular modelling for drug development in therapeutic targets as shown in (Figs 5-7). The ligands and receptor have

PROTEIN : 8D59 (METT1)
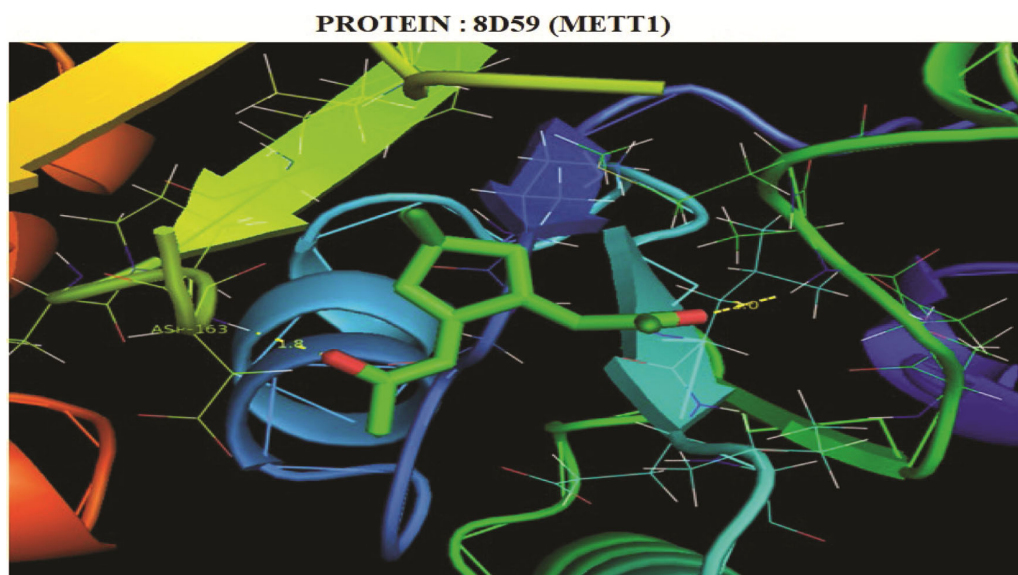
Fig. 6 — Ligand -protein interactions of anti-cancer compound identified from *Aegle marmelos* within the active site of METT1 (2a) 1-(3, 6, 6-trimethyl-1, 6, 7, 7a-tetrahydrocyclopenta[c]pyran-1-yl)ethanone

PROTEIN : 8D59 (METT1)
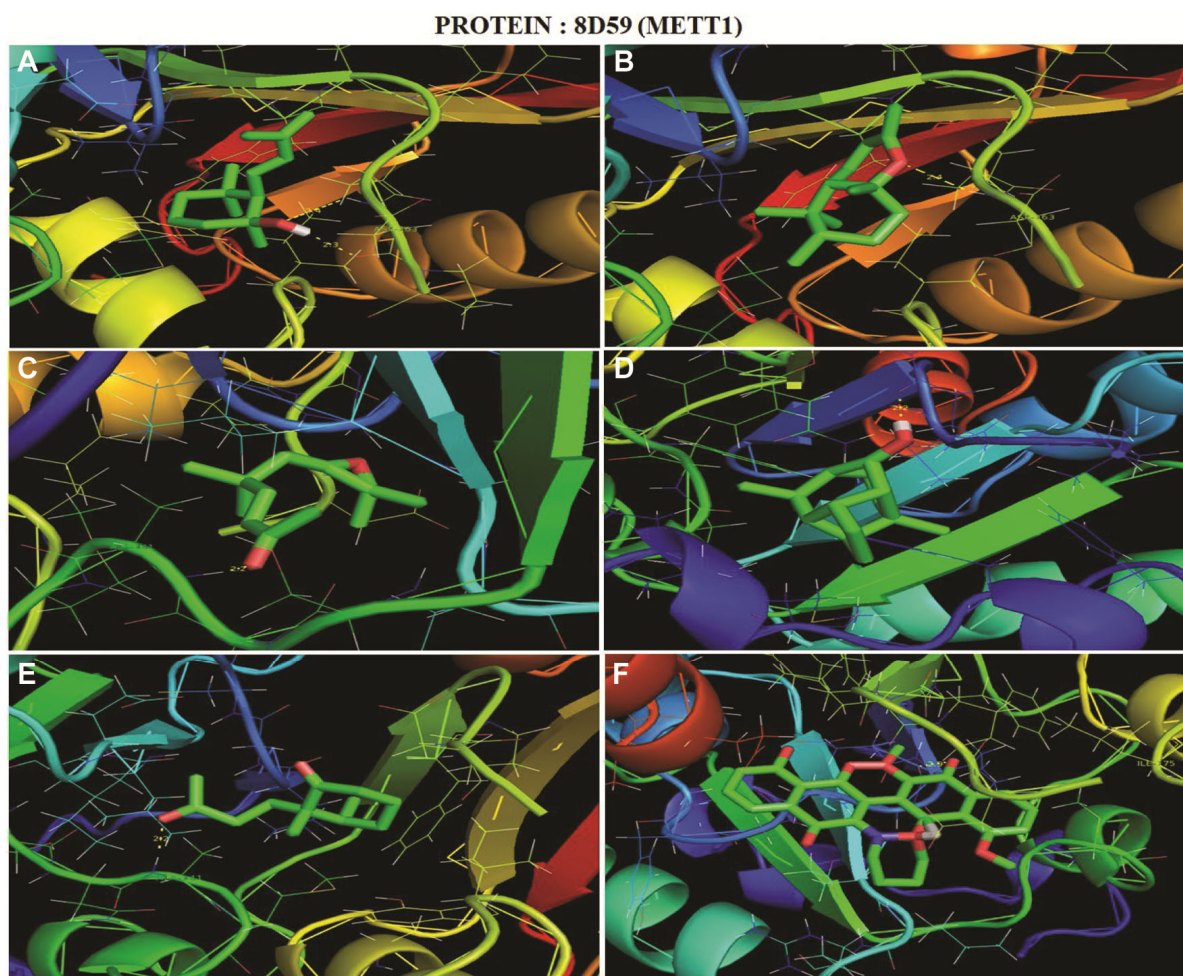
Fig. 7 — (*Contd.*)
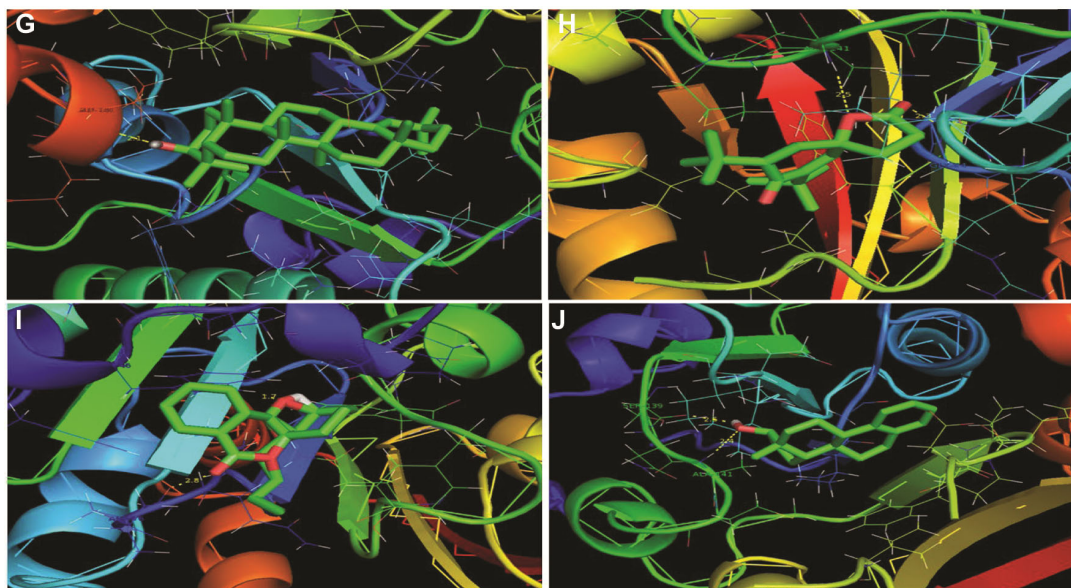
Fig. 7 — Ligand -protein interactions of anti-cancer compounds identified from *Calotropis gigantea* within the active site of METT1 (3a)1-cyclohexanol, 2-(3-methyl-1, 3-butadienyl)-1, 3, 3-trimethyl-; (3b)2, 5, 5, 6, 8a-pentamethyl-trans-4a, 5, 6, 7, 8, 8a-hexahydro-gamma-chromene;(3c)6-(3,   3-dimethyl-oxiran-2-ylidene)-5,   5-dimethyl-hex-3-en-2-one;(3d)1,   4-Methanoazulene-9-methanol, decahydro-4, 8, 8-trimethyl-, [1S-(1α, 3aβ, 4α, 8aβ, 9R*)]-; (3e)cyclohexanone, 2, 3-dimethyl-2-(3-oxobutyl)-; (3f)3', 8, 8'-trimethoxy-3-piperidyl-2, 2'-binaphthalene-1, 1', 4, 4'-tetrone; (3g)7, 9-di-tert-butyl-1-oxaspiro (4, 5)deca-6, 9-diene-2, 8-dione; (3h)germanicol; (3i)1, 2-benzenedicarboxylic acid, butyl cyclohexyl ester; and (3j)estra-1, 3, 5(10)-trien-17β-ol

been downloaded and converted as PDB file format for dock tiny molecules with receptor performed by AutoDock 4.2 program and the docking result used to visualize by PyMol software[37]. After the hydrogen and kollman charges are added, set several torsion for converting PDBQT format by run autogrid and autodock, which express ten conformations of ligand - protein interaction. The resulting docking identifies the best binding conformation, hydrogen bond interactio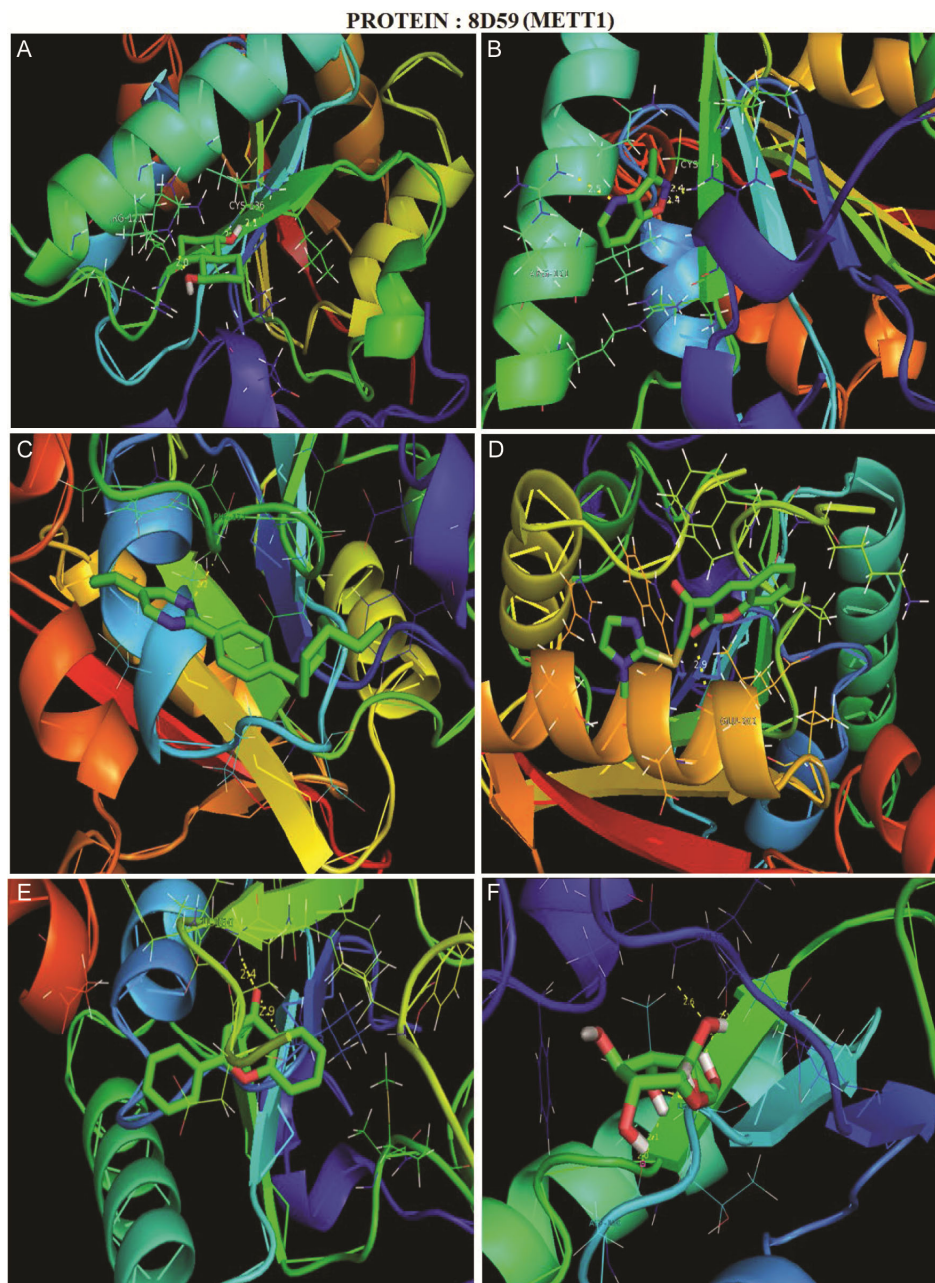n with amino acid residues, inhibition constant and intermolecular energy as listed (Table 5). The ligplot of 8D59 (METTL1) and ligand interaction expressed the dashed line associated with different kinds of bonds, such as carbon-hydrogen, pi-cation, pi-alkyl, pi-sigma and hydrogen bond between the donor and acceptor[38]. These interactions can be impacted by electrostatic forces, steric, weak and Van der Waals effect, which establish the biological properties and effectiveness of the synthesized compounds[39]. The anti-tumor demonstrates the strongest binding affinity was located from -4.47 to -8.83kcal/mol. The most of the components 1c, 1e, 2a, 3b, 3d, 3f, 3g, 3h, 3i, 3j, which have estimated binding energies smaller than other compounds[40]. Among the all compounds the lowest binding affinity expressed in the 3', 8, 8'-Trimethoxy-3-piperidyl-2, 2'-binaphthalene-1, 1', 4, 4'-tetrone (-8.83 kcal/mol) and

Germanicol (-8.27 kcal/mol) with bonded residues (ILE 83, GLU 240) and hydrogen interaction (O…HN, O…O) from ligand (donor) to receptor (acceptor), that compound identified from the extract of *Calotropis gigantean.* Finally, we report the high content of anti-cancer compounds present in flower of *Calotropis gigantean* greater than leaves of *Hybanthus enneaspermus, Aegle marmelos.* These results indicate the potential for the creation novel and effective drug development to treat cancer illness, respectively.

Drug-likeness and ADME properties analysis

The theoretical approach of drug-likeness is used to predict various physiochemical properties and pharmacokinetics of potential drug candidates, which reduces time and expense in the process of developing drugs for the body of the person. The five rules have been applied to evaluate the oral absorption of bulk compounds and examine their drug-likeness qualities, which result revealed no violation of the human body[41]. In the present investigation, drug-likeness has crucial in the drug-discovery process, which has examined the seventeen compounds based on Lipinski rule of five interpreted by using online server pkCSM – Biosig lab as listed in (Table 6), it was found all components are indicate no violations of human body, which include molecular mass<500, HBA<10,

Table 5 — The docking scores of seventeen phytochemicals interaction with the receptor METT1

Compound name	Bonded residues	Hydrogen bond interactions (ligand protein)	Bond distance (Å)	No. of hydrogen bond	Estimated inhibition constant (μm)	Binding energy (kcal/mol)	Reference RMSD (Å)
1, 5-naphthalenediol, decahydro-	ARG 121	O…HE	2.0	3	232.82	-4.96	43.28
	CYS 136	O…HN	2.1				
	CYS 136	H…O	2.1				
3-Methylisoxazolo [4, 5-b]pyridine	ARG 121	N…1HH2	2.5	3	525.18	-4.47	43.90
	CYS 136	N…HN	2.4				
	CYS 136	O…HN	2.4				
Pyrimidine, 5-ethyl-2-[4-(4-ethylcyclohexyl) phenyl]	PHE 131	N…HN	2.2	1	68.77	-5.68	35.66
Coumarine, 3-[2-(1-methyl-2-imidazolylthio)-1-oxoethyl]	GLU 202	O…O	2.9	1	273.82	-4.86	80.11
Flavone	LEU 160	O…HN	2.4	2	51.99	-5.84	39.80
	ILE 83	O…O	2.9				
Glucose	GLN 77	H…O	2.1	7	92.90	-4.51	65.40
	GLN 77	H…O	2.0				
	GLN 77	O…HN	2.6				
	LEU 102	O…HN	1.6				
		O…HN	2.6				
	ASP 100	H…O	2.1				
		H…O	2.0				
1-(3, 6, 6-Trimethyl-1, 6, 7, 7a-tetrahydrocyclopenta[c]pyran-1-yl)ethanone	ASP 163	O…HN	1.8	2	97.08	-5.47	41.62
	ALA 141	O…HN	2.0				
1-Cyclohexanol, 2-(3-methyl-1, 3-butadienyl)-1, 3, 3-trimethyl-	ASP 163	H…O	2.3	2	181.47	-5.10	41.70
	ASP 163	O…HN	2.4				
2, 5, 5, 6, 8a-Pentamethyl-trans-4a, 5, 6, 7, 8, 8a-hexahydro-gamma-chromene	ASP 163	O…HN	2.4	1	53.62	-5.83	42.03
6-(3, 3-Dimethyl-oxiran-2-ylidene)-5, 5-dimethyl-hex-3-en-2-one	ALA 141	O…HN	2.2	1	189.27	-5.08	42.75
1, 4-Methanoazulene-9-methanol, decahydro-4, 8, 8-trimethyl-, [1S-(1α, 3aβ, 4α, 8aβ, 9R*)]-	GLN 77	H…OE1	2.2	1	67.02	-5.69	25.87
Cyclohexanone, 2, 3-dimethyl-2-(3-oxobutyl)-	ALA 141	O…HN	2.2	1	197.95	-5.05	41.75
3', 8, 8'-Trimethoxy-3-piperidyl-2, 2'-binaphthalene-1, 1', 4, 4'-tetrone	ILE 83	O…O	2.9	1	334.16	-8.83	39.38
7, 9-Di-tert-butyl-1-oxaspiro(4, 5)deca-6, 9-diene-2, 8-dione	GLY 84	O…HN	2.3	2	28.74	-6.20	40.16
	ALA 141	O…HN	2.5				
Germanicol	GLU 240	O…HN	2.1	1	872.52	-8.27	43.54
1, 2-Benzenedicarboxylic acid, butyl cyclohexyl ester	ALA 76	O…O	2.8	2	18.02	-6.47	25.55
	TRP 46	O…HE1	1.7				
Estra-1, 3, 5(10)-trien-17β-ol	SER 139	H…O	2.5	2	16.02	-6.54	42.11
	ALA 141	O…HN	2.4				

HBD<05, logP<5 and PS <140 of the novel compounds was identified from *Hybanthus enneaspermus, Aegle marmelos* leaves & *Calotropis gigantea* flowers. The calculated drug-likeness of all anti-tumour compounds satisfied five rules except the germanicol of the natural compound. The drug-likeness criteria are connected with ADME properties of water solubility, Caco2 cell line (Caucasian colon adenocarcinoma) is a absorption, which express the Caco2 permeability of human epithelial. The translate

Table 6 — Drug-likeness and ADME properties of seventeen phytochemicals

Properties	MW g/mol	Log P	HBD	HBA	Water Solubility	Caco2 permeability	skin permeability	PSA(Å^2)
Lipinski 5 rule's & ADME	<500	<5	<5	<10	-	-	-	<130
3-Methylisoxazolo [4, 5-b] pyridine	134.13	1.531	0	3	-1.11	1.84	-2.28	57.66
1, 5-naphthalenediol, decahydro-	170.25	1.308	2	2	-1.49	1.57	-3.65	73.60
Pyrimidine, 5-ethyl-2-[4-(4-ethylcyclohexyl) phenyl]	294.44	5.389	0	2	-5.47	1.33	-2.44	133.57
Coumarine, 3-[2-(1-methyl-2-imidazolylthio)-1-oxoethyl]	300.33	2.501	0	6	-2.88	0.98	-2.79	124.15
Flavone	222.24	3.460	0	2	-3.83	1.26	-2.21	98.13
Glucose	180.15	-3.220	5	6	-1.37	-0.24	-3.04	68.64
1-(3, 6, 6-Trimethyl-1, 6, 7, 7a-tetrahydrocyclopenta[c]pyran-1-yl)ethanone	206.28	2.850	0	2	-3	1.62	-2.49	91.00
1-Cyclohexanol, 2-(3-methyl-1, 3-butadienyl)-1, 3, 3-trimethyl-	208.34	3.553	1	1	-4.43	1.51	-1.54	93.89
2, 5, 5, 6, 8a-Pentamethyl-trans-4a, 5, 6, 7, 8, 8a-hexahydro-gamma-chromene	208.34	4.141	0	1	-4.14	1.52	-2.04	93.89
6-(3, 3-Dimethyl-oxiran-2-ylidene)-5, 5-dimethyl-hex-3-en-2-one	194.27	2.850	0	2	-3.20	1.34	-3.18	85.644
1, 4-Methanoazulene-9-methanol, decahydro-4, 8, 8-trimethyl-, [1S-(1α, 3aβ, 4α, 8aβ, 9R*)]-	222.37	3.467	1	1	-4.20	1.29	-2.16	99.62
Cyclohexanone, 2, 3-dimethyl-2-(3-oxobutyl)-	196.29	2.751	0	2	-2.30	1.33	-2.37	86.07
3', 8, 8'-Trimethoxy-3-piperidyl-2, 2'-binaphthalene-1, 1', 4, 4'-tetrone	487.50	3.802	0	8	-4.97	1.07	-2.78	107.67
7, 9-Di-tert-butyl-1-oxaspiro (4, 5) deca-6, 9-diene-2, 8-dione	276.37	3.589	0	3	-4.24	1.4	-2.72	120.62
Germanicol	426.72	8.168	1	1	-6.63	1.22	-2.84	192.39
1, 2-Benzenedicarboxylic acid, butyl cyclohexyl ester	304.38	4.133	0	4	-4.44	1.42	-2.78	131.35
Estra-1, 3, 5(10)-trien-17β-ol	256.38	3.903	1	1	-4.90	1.66	-2.48	115.58

predicted value is greater than 0.90 and all the components are satisfied this conditions. Skin permeability has been estimated by the same server for drug development after following effective molecular docking results, which estimates the first step of bioavailability of compounds, respectively.

The geometry optimized structures

The optimized structure demonstrates topology, size, shape, and the stability of the molecular structure in the chemical process for drug design and the prediction of complex behaviour of atomic-scale with lowest ground state energy is done by density functional theory, which contributes to the cost-effective, improved efficiency and a higher quality result of the molecular system. The geometry-optimized structure of seventeen anti-cancer components have been identified from extract of *Hybanthus enneaspermus*, *Aegle marmelos* and *Calotropis gigantea* were estimated by Gaussian 09W hybrid functional DFT/B3LYP/6-311++G (d, p) approach[42] as shown in (Figs 8-10). The bond angle and bond length have been visualized by Chemcraft application using with.log file, which file optimized from ChemDraw Ultra software[43]. In VSERPR theory, the distance between the nuclei of two atoms that are covalently connected is known as bond length. The angle created between two covalent bonds made by the same atom is known as a bond angle, any two neighbouring covalent bonds can generate a bond angle, which is an optimized geometric angle. The bond length act based on bond order that describes the number of electrons (single bond, double bond and triple bond). The number of electron pairs increased among the bond distance, and the stability of the bond also increased
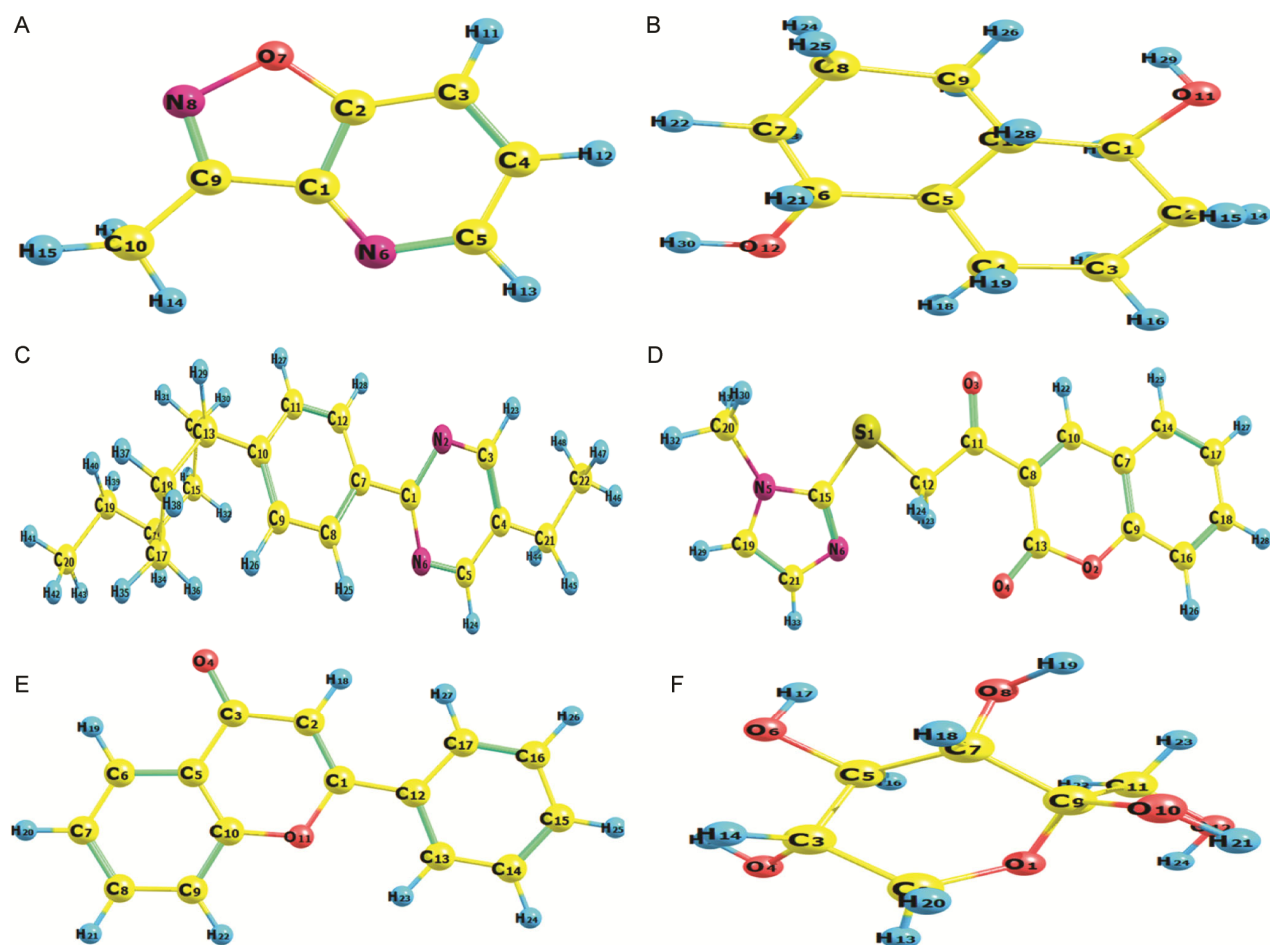
Fig. 8 — Geometry optimized structure with numbering system of phytochemicals identified from *Hybanthus enneaspermus* (1a)3-methylisoxazolo [4, 5-b] pyridine; (1b) 1, 5-naphthalenediol, decahydro-; (1c) pyrimidine, 5-ethyl-2-[4-(4-ethylcyclohexyl) phenyl]; (1d)coumarine, 3-[2-(1-methyl-2-imidazolylthio)-1-oxoethyl]; (1e) flavone; and (1e)glucose
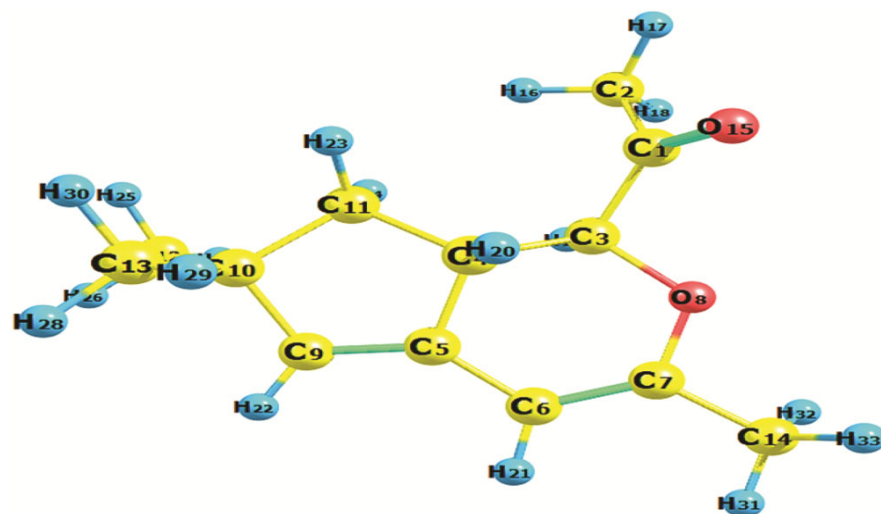
Fig. 9 — Geometry optimized structure with numbering system of phytochemicals identified from *Aegle marmelos* (2a)1-(3, 6, 6-Trimethyl-1, 6, 7, 7a-tetra hydrocyclopenta[c]pyran-1-yl) ethanone
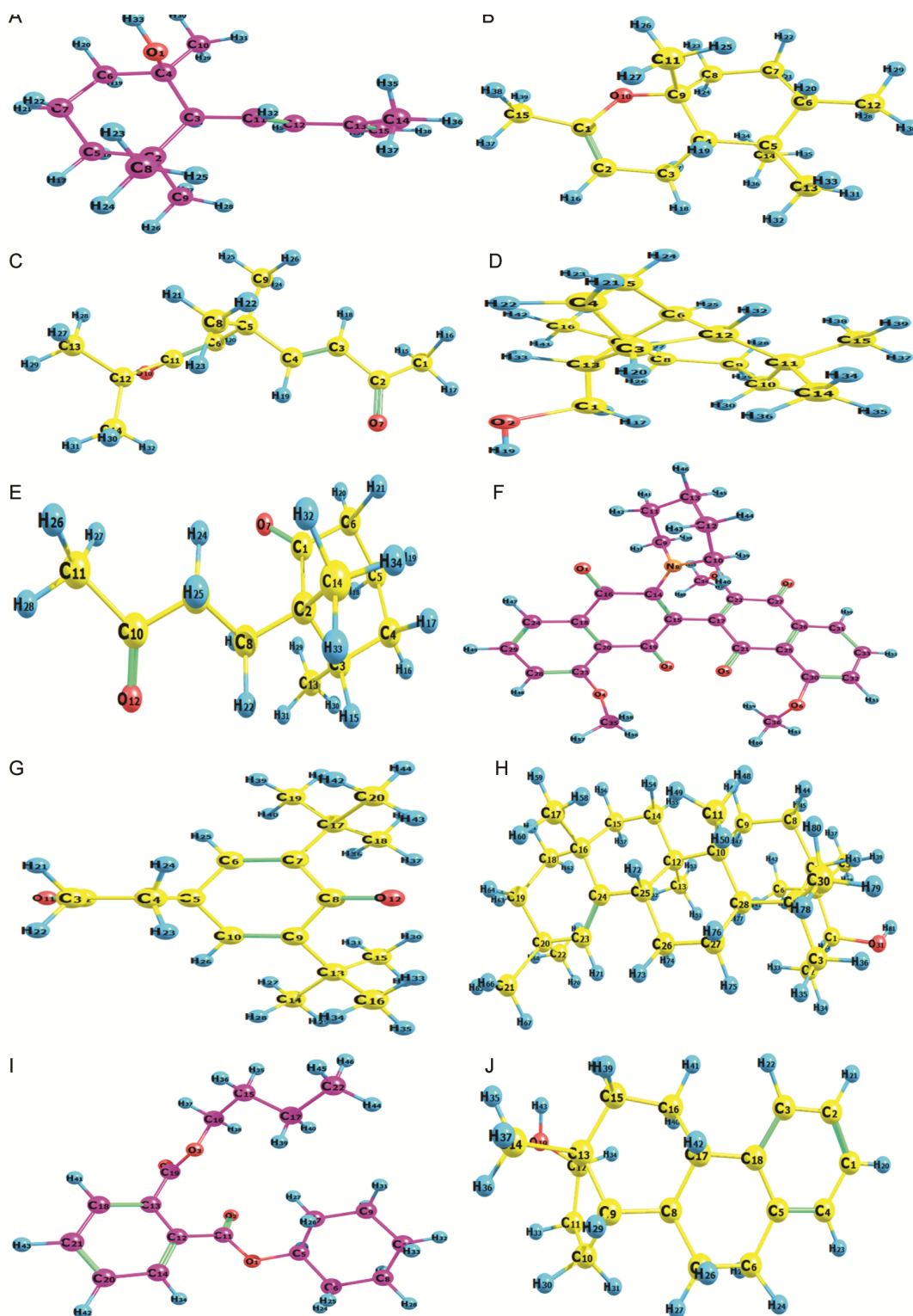
Fig. 10 — Geometry optimized structure with numbering system of phytochemicals identified from *Calotropis gigantea*(3a)1-cyclohexanol, 2-(3-methyl-1, 3-butadienyl)-1, 3, 3-trimethyl-; (3b)2, 5, 5, 6, 8a-pentamethyl-trans-4a, 5, 6, 7, 8, 8a-hexahydro-gamma-chromene; (3c)6-(3, 3-dimethyl-oxiran-2-ylidene)-5, 5-dimethyl-hex-3-en-2-one; (3d)1, 4-methanoazulene-9-methanol, decahydro-4, 8, 8-trimethyl-, [1S-(1α, 3aβ, 4α, 8aβ, 9R*)]-; (3e)cyclohexanone, 2, 3-dimethyl-2-(3-oxobutyl)-; (3f)3', 8, 8'-Trimethoxy-3-piperidyl-2, 2'-binaphthalene-1, 1', 4, 4-tetrone; (3g)7, 9-Di-tert-butyl-1-oxaspiro (4, 5)deca-6, 9-diene-2, 8-dione; (3h)Germanicol; (3i)1, 2-Benzenedicarboxylic acid, butyl cyclohexyl ester; and (3j)estra-1, 3, 5(10)-trien-17β-ol

Table 7 — The bond angle and bond length of optimized geometry structure for seventeen bio-compounds obtain by B3LYP/6-311++G (d, p)

Compound name	Bond length low (Å)	Bond length high (Å)	Bond angle low (°)	Bond angle high (°)
3-Methylisoxazolo [4, 5-b] pyridine	$(C_3-H_{11}) \rightarrow 1.084$	$(C_9-C_{10}) \rightarrow 1.497$	$(C_2-C_1-C_9) \rightarrow 103.82$	$(N_6-C_1-C_9) \rightarrow 131.27$
1, 5-naphthalenediol, decahydro-	$(O_{11}-H_{29}) \rightarrow 0.963$	$(C_1-C_{10}) \rightarrow 1.535$	$(C_2-C_1-O_{11}) \rightarrow 105.74$	$(C_{10}-C_1-O_{11}) \rightarrow 111.36$
Pyrimidine, 5-ethyl-2-[4-(4-ethylcyclohexyl) phenyl]	$(C_{11}-H_{27}) \rightarrow 1.100$	$(C_{13}-C_{14}) \rightarrow 1.526$	$(C_{44}-C_{21}-O_{45}) \rightarrow 106.74$	$(N_2-C_1-N_6) \rightarrow 124.53$
Coumarine, 3-[2-(1-methyl-2-imidazolylthio)-1-oxoethyl]	$(C_{19}-H_{29}) \rightarrow 1.077$	$(S_1-C_{12}) \rightarrow 1.834$	$(C_{12}-S_1-C_{15}) \rightarrow 97.042$	$(C_{21}-C_{19}-H_{29}) \rightarrow 132.58$
Flavone	$(C_9-H_{22}) \rightarrow 1.098$	$(C_3-C_5) \rightarrow 1.469$	$(O_{11}-C_1-C_{12}) \rightarrow 111.134$	$(C_2-C_1-C_{12}) \rightarrow 126.01$
Glucose	$(O_8-H_{19}) \rightarrow 0.965$	$(O_1-O_{12}) \rightarrow 2.744$	$(O_1-O_{12}-H_{24}) \rightarrow 58.85$	$(C_2-O_1-O_{12}) \rightarrow 170.77$
1-(3, 6, 6-Trimethyl-1, 6, 7, 7a-tetrahydrocyclopenta[c]pyran-1-yl)ethanone	$(C_6-H_{21}) \rightarrow 1.084$	$(C_{10}-C_{11}) \rightarrow 1.564$	$(C_9-C_{10}-C_{11}) \rightarrow 101.27$	$(C_6-C_5-C_9) \rightarrow 132.69$
1-Cyclohexanol, 2-(3-methyl-1, 3-butadienyl)-1, 3, 3-trimethyl-	$(O_7-H_{23}) \rightarrow 0.964$	$(C_1-C_2) \rightarrow 2.744$	$(C_1-C_2-H_{16}) \rightarrow 106.87$	$(C_{11}-C_{12}-C_{13}) \rightarrow 170.77$
2, 5, 5, 6, 8a-Pentamethyl-trans-4a, 5, 6, 7, 8, 8a-hexahydro-gamma-chromene	$(C_2-H_{16}) \rightarrow 1.094$	$(C_4-C_5) \rightarrow 1.547$	$(C_8-C_{19}-H_{10}) \rightarrow 102.61$	$(C_2-C_1-C_{15}) \rightarrow 126.79$
6-(3, 3-Dimethyl-oxiran-2-ylidene)-5, 5-dimethyl-hex-3-en-2-one	$(C_3-H_{18}) \rightarrow 1.101$	$(C_5-C_9) \rightarrow 1.525$	$(C_4-C_5-C_6) \rightarrow 107.66$	$(C_6-C_{11}-C_{12}) \rightarrow 161.76$
1, 4-Methanoazulene-9-methanol, decahydro-4, 8, 8-trimethyl-, [1S-(1α, 3aβ, 4α, 8aβ, 9R*)]-	$(O_2-H_{19}) \rightarrow 0.963$	$(C_9-H_{18}) \rightarrow 3.327$	$(H_{18}-C_{10}-H_{30}) \rightarrow 30.94$	$(O_2-C_1-C_{10}) \rightarrow 171.00$
Cyclohexanone, 2, 3-dimethyl-2-(3-oxobutyl)-	$(C_{11}-H_{28}) \rightarrow 1.116$	$(C_2-C_3) \rightarrow 1.543$	$(H_{16}-C_4-H_{17}) \rightarrow 106.92$	$(C_9-C_{10}-O_{12}) \rightarrow 122.97$
3', 8, 8'-Trimethoxy-3-piperidyl-2, 2'-binaphthalene-1, 1', 4, 4'-tetrone	$(C_{17}-C_{41}) \rightarrow 1.124$	$(C_{14}-C_{15}) \rightarrow 1.511$	$(O_{22}-C_{11}-H_{43}) \rightarrow 90.54$	$(N_{25}-O_{22}-H_{44}) \rightarrow 134.33$
7, 9-Di-tert-butyl-1-oxaspiro (4, 5)deca-6, 9-diene-2, 8-dione	$(C_{19}-H_{39}) \rightarrow 1.116$	$(C_4-C_5) \rightarrow 1.552$	$(C_2-C_3-C_4) \rightarrow 104.84$	$(C_3-C_2-O_{11}) \rightarrow 132.22$
Germanicol	$(C_{31}-H_{81}) \rightarrow 0.964$	$(C_1-C_4) \rightarrow 1.546$	$(C_{29}-C_{28}-H_{77}) \rightarrow 103.57$	$(C_{11}-C_{50}-H_{78}) \rightarrow 130.57$
1, 2-Benzenedicarboxylic acid, butyl cyclohexyl ester	$(C_{20}-H_{41}) \rightarrow 1.113$	$(C_{14}-C_{15}) \rightarrow 1.523$	$(O_9-C_{18}-H_{38}) \rightarrow 88.70$	$(C_{13}-O_9-C_{18}) \rightarrow 153.51$
Estra-1, 3, 5(10)-trien-17β-ol	$(O_{19}-H_{43}) \rightarrow 0.964$	$(C_{12}-C_{13}) \rightarrow 1.551$	$(C_9-C_{13}-C_{12}) \rightarrow 103.64$	$(C_6-C_5-C_{18}) \rightarrow 122.13$

inversely proportional to the number of electron pairs decrease among the bond distance, the stability of the bond also reduced[44]. The optimized structure of seventeen compounds reports the small bond length indicates the strongest bond and the high bond length is associated with the weakest bond of molecular structure. If the bond angle is smaller, the surrounding pair of bonds is very strong and repulsive strength leads to high electron density. The higher bond angle indicates greater electronegativity variation among the atoms, which strengthens the dipole moment[45]. Therefore, 3-Methylisoxazolo [4, 5-b] pyridine expressed the low bond length$(C_3-H_{11}) \rightarrow 1.084$Å and high bond length $(C_9-C_{10}) \rightarrow 1.497$Å while the lowest bond angle$(C_2-C_1-C_9) \rightarrow 103.82°$ and highest bond length $(N_6-C_1-C_9) \rightarrow 131.27°$ and remain compounds bond length, bond angle values as given in (Table 7). The optimized structure of compounds reports the small bond angle to

represent the nearby lone pair and bond pair expresses the strong repulsion towards increased electron density and the high bond angle indicates the different electronegative and strongest dipole moment in the molecules, respectively.

Conclusion

In this work, the Phytoconstituents compounds identified from an extract of *Hybanthus enneaspermus, Aegle marmelos* and *Calotropis gigantea* were evaluated by GC-MS analysis. The result of GC-MS revealed seventeen anti-cancer compounds from forty-four bio-components. The molecular docking examined seventeen cancer compounds dock with receptor METTL1 (8D59), which expressed strong binding affinity of 3', 8, 8'-Trimethoxy-3-piperidyl-2, 2'-binaphthalene-1, 1', 4, 4'-tetrone $\rightarrow$ (-8.83 kcal/mol). The evaluated drug-likeness of all anti-cancer compounds

satisfied the Lipinski rule of five except the germanicol compound. ADME properties also calculated the physiochemical properties and pharmacokinetics for drug development. The geometry-optimized structure, bond length and bond angle of seventeen anti-cancer components have been predicted for structure conformation to describe the stability and complex behaviour of molecules. The above-evaluated computational drug design approaches contribute by cost-effective, time-consuming, enhanced efficiency and quality of drug development of new therapeutic targets and medication candidates as quickly as practicable.

Conflict of interest
All authors declare no conflict of interest.

References
1   Shivangi G, Nidhi G, Sreemoyee C & Surendra N, Natural plant extracts as potential therapeutic agents for the treatment of cancer. *Curr Top Med Chem,* 17 (2017) 96.
2   Chinaza GA & Hannington T, The Medical, pharmaceutical & nutritional biochemistry and uses of some common medicinal plants. *Medicinal and Aromatic Plants of the World (MAPs),* 2021.
3   Han CV, Rajeev B & Gulam R, Flower extracts and their essential oils as potential antimicrobial agents for food uses and pharmaceutical applications. *CRFSFS,* 11 (2012) 00169.
4   Ananthapalpu Krishnan NR & Rengasamy DA, Current pharmacological impacts and perspective of *Hybanthus enneaspermus* (Linn.) F. Muell. *Pharmacogn Res,* 14(2022) 342.
5   Ahmad W, Amir M, Ahmad A, Ali A, Ali A, Wahab S, Barkat HA, Ansari MA, Sarafroz M, Ahmad A, Barkat A, Alam P, *Aegle marmelos* Leaf Extract Phytochemical Analysis, Cytotoxicity, *In vitro* Antioxidant and Antidiabetic Activities. *Plants,* 10 (2021) 2573.
6   Sreewardhini S, Sankari D, Vijayalakshmi V, Mangalagowri A & Veeramuthu A, Phytochemical analysis, anti-inflammatory, antioxidant activity of *Calotropis gigantea* and its therapeutic applications. *J Ethnopharmacol,* 303 (2023) 115963.
7   Sand hanasamy D & MohamadAlSalhiS, Identification, evaluation the source of natural bioactive compounds from *Calotropis gigantea* L. flowers and their anticancer potential. *J King Saud Univ Sci,* 36 (2024) 103038.
8   Wenli C, Aili G, Hui L, Wenjuan Z, Novel roles of METTL1/WDR4 in tumor*via* m7G methylation. *MolTherOncolytics,* 26 (2022) 009.
9   Halil S, Ahmet GA, Sezen A, Nuray UG, Synthesis, characterization, molecular docking and *in vitro* anti-cancer activity studies of new and highly selective 1, 2, 3-triazole substituted 4-hydroxybenzohyrdazide derivatives. *J Mol Struct*, 1283 (2023) 135247.
10 Yu Z, Xing Z, Lei Q, Zimei D, Xiaojing H, BaofuQ, Jirong S, Jie H, Synthesis, structures, drug-likeness, *In vitro* evaluation and *in silico* docking on novel N-benzoyl-N′-phenyl thiourea derivatives. *J Mol Struct,* 1176 (2019) 335.
11 Lawrence M, Rajesh P, Thirunavukkarasu M, Muthu S, Solute-solvent interactions, electrostatic & covalent surface analysis, and pharmacokinetic studies *via in silico* simulation on diethyl 3-hydroxyglutarate: Anti-hypercholesterolemia activity. *J Mol Liq,* 382 (2023) 121940.
12 Sangeetha K, Swaminathan C, Renuka R, Vellaikumar S, Nivethadevi P, Sivasankari B, GC–MS profiling of phytocompounds in the leaves of *Vitex negundo* L. *Curr Sci,* 125 (2023) 250.
13 FrancaCM, Donatella G, Luisa L, Chapter-5.7-Five-Membered Ring Systems with O & N Atoms. *Adv Heterocycl Chem,* 26 (2014) 319.
14 Lan L, Jing JJ, Qiu Z, Xue Z, Shilong Z, Guangdi W, Ling H, Synthesis and anticancer activityevaluation of naphthalene-substituted triazolespirodienones. *Eur J Med Chem,* 5 (2021) 113039.
15 Beata T, Benita W, Zaneta C, Aneta CN, Elzbieta G, Anna JK, Novel Pyrimidine Derivatives as Potential Anticancer Agents: Synthesis, Biological Evaluation and Molecular Docking Study.*Int J Mol Sci,* 22 (2021) 825.
16 Narayan B, Anupa KA, Yuba RP, Paras NY, Anticancer Potential of Coumarin and its Derivatives, *Mini Rev Med Chem,* 21 (2021) 19.
17 Dalia MK, Valdas J, Arunas S, Jurga B, Flavonoids as Anticancer Agents. *Nutrients,* 12 (2020) 12020457.
18 Farag MA, Gad MZ, Omega-9 fatty acids: potential roles in inflammation and cancer management. *J Genet Eng Biotechnol,* 20 (2022) 48.
19 Adewale F, Basiru A, Oluwafemi O, Olusola A, Israel OO, Rosemary E, Biology of glucose metabolization in cancer cells. *J Oncol Sci,* 3 (2017) 45.
20 Alexand ru OD, Romeo CT, Florin M, Eugenia D, Janos D, Kalman I, Marius B, Daliborca CV, Roxana P, Adinela C & Dana CB, The Role of Methyl-(Z)-11-tetradecenoate Acid from the Bacterial Membrane Lipid Composition in *Escherichia coli* Antibiotic Resistance. *Biomed Res Int,* 2022 (2022) 6028045.
21 Mohamed TS, Mohamed FG, Sara MF, Antibacterial activities of hexadecanoic acid methyl ester and green synthesized silver nanoparticles against multidrug-resistant bacteria. *J Basic Microbiol,* 61 (2021) 061.
22 Xiao G, Peng Q, Benqiong G, Yixin Z, Zhihao F, Decai Y, Chunmei Z, Yang C, Jingbin N, Jianghong L, Jin Z, ailian S, Guoping L, Heptadecanoic acid and pentadecanoic acid crosstalk with fecal-derived gut microbiota are potential noninvasive biomarkers for chronic atrophic gastritis. *Front Cell Infect Microbiol,* 12 (2023) 737.
23 Paramasivan M, Gangatharan M & Nainangu PB, Prediction aided *In vitro* analysis of octa-decanoic acid from *Cyanobacterium Lyngbya* sp. as a proapoptotic factor in eliciting anti-inflammatory properties. *Bioinformation,* 13 (2017) 301.
24 Gomes ACS, Demuner AJ, Alvarenga ES, Gondim JPE, Fonseca AR, Buonicontro DS, Pilau EJ & Silva E, Synthesis and Evaluation of Nematicidal Activity of Compound Derived from Norbornadiene. *J Braz Chem Soc*, 31 (2020) 1805.
25 Mohamed HS, Abdelgawad MA, Hegab M, Hamza ZS, Nagdy AM, Ahmed SA, Ahmed OM, Ghoneim MM, Computational and Molecular Docking Studies of New Benzene Sulfonamide Drugs with Anticancer and Antioxidant Effects. *Curr Org Synth*, 20 (2023) 339.

26 Soon YS, Jihyun P, Yearam J, Young HL, Dongsoo K, Youngdae Y & Yoongho L, Anticancer activities of cyclohexenone derivatives. *Appl Biol Chem,* 82 (2020) 63.

27 Kyriakopoulos CE, Heath EI, Eickhoff JC, Kolesar J, Yayehyirad M, Moll T, Wilding G, Liu G, A multicenter phase 1/2a dose-escalation study of the antioxidant moiety of vitamin E 2, 2, 5, 7, 8-pentamethyl-6-chromanol (APC-100) in men with advanced prostate cancer. *Invest New Drugs,* 34 (2016) 225.

28 Nishant KR, Rahul BS & Sangeeta VJ, Potential 2, 4-dimethyl-1H-pyrrole-3-carboxamide bearing benzimidazole template: Design, synthesis, *In vitro* anticancer and *in silico* ADME study. *Bioorg Chem,* 97 (2020) 103660.

29 Zhou L, Li X, Chen X, Li Z, Liu X, Zhou S, Zhong Q, Yi T, Wei Y, Zhao X, Qian Z, *In vivo* antitumor and antimetastatic activities of camptothecin encapsulated with N-trimethyl chitosan in a preclinical mouse model of liver cancer. *Cancer Lett,* 297 (2010) 56.

30 Vera de LA, Claudia GS, And reia FS, Priscilla RVC, Kenn F, Julio CDL, Luc P, Aspidosperma species: A review of their chemistry and biological activities. *J Ethnopharmacol,* 231 (2019) 125.

31 Yang Y, Wu H, Zou X, Chen Y, He R, Jin Y, Zhou B, Ge C, Yang Y, A novel synthetic chalcone derivative, 2, 4, 6-trimethoxy-4′-nitrochalcone (Ch-19), exerted anti-tumor effects through stimulating ROS accumulation and inducing apoptosis in esophageal cancer cells. *Cell Stress Chaperones*, 27 (2022)645.

32 Yugand har D, Lakshma NV, Sivakumar A, Kunta CS, Ajay KS, Design, synthesis and anticancer properties of novel oxa/azaspiro[4, 5]trienones as potent apoptosis inducers through mitochondrial disruption. Eur. *J Med Chem,* 101 (2015) 348.

33 Hu YL, Wang XB, Chen DD, Guo XJ, Yang QJ, Dong LH, Cheng L, Germanicol induces selective growth inhibitory effects in human colon HCT-116 and HT29 cancer cells through induction of apoptosis, cell cycle arrest and inhibition of cell migration. *JBUON*, (2016) 626.

34 Krishnan K, Mani A & Jasmine S, Cytotoxic Activity of Bioactive Compound 1, 2- Benzene Dicarboxylic Acid, Mono 2- Ethylhexyl Ester Extracted from a Marine Derived Streptomyces sp. VITSJK8. *Int J Mol Cell Med,* 3 (2014) 246.

35 Abou-Salim MA, Shaaban MA, Abd El HMK, Alanazi MM, Hala WF & Elshaier YAMM, Utilizing Estra-1, 3, 5, 16-Tetraene Scaffold: Design and Synthesis of Nitric Oxide Donors as Chemotherapeutic Resistance Combating Agents in Liver Cancer. *Molecules,* 28 (2023) 754.

36 Esteban OA, Qi L, Eliza Y, Mehdi P, Etienne DB, Wencai Z, Jihoon L, Demetrios A, Erdem S, Dimitrios AG, Muxin G,

Raja A, Alejand ro G, Sigitas M, Gonçalo JLB, Eric SF, Allan B, George SV, Frank JS, Konstantinos T, Richard IG, METTL1-mediated m7G modification of Arg-TCT tRNA drives oncogenic transformation. *Mol Cell,* 81 (2021) 3323.

37 ShivarajRB, Raveendra M, SudhirHM, Raviraj. K, Seema SK, Christopher JS, Synthesis, spectroscopic (FT-IR, FT-Raman, NMR & UV-Vis), reactive (ELF, LOL, Fukui), drug likeness and molecular docking insights on novel 4-[3-(3-methoxy-phenyl)-3-oxo-propenyl]-benzonitrile by experimental and computational methods. *Heliyon,* 7 (2021) e08429.

38 SudhirHM, MahanteshaBM, SeemaKS, Ashwini R, Anurag RM, Varsha KV, Mahesh RT, Christopher JS, Structural, vibrational, fluorescence spectral features, Hirshfeld surface analysis, docking and drug likeness studies on 4-(2-bromo-4-methyl-phenoxymethyl)-6-methyl-coumarin derivative: Experimental and theoretical studies. *J Photochem Photobiol A: Chem*, 431 (2022) 114055.

39 Eze AA, Obinna GC, Eyuwa AI, Bassey EO, Daniel AC, Sopuruchukwu OE, Innocent Benjamin, Hitler Louis, Structural analysis, reactivity descriptors (HOMO-LUMO, ELF, NBO), effect of polar (DMSO, EtOH, H2O) solvation, and libido-enhancing potential of resveratrol by molecular docking. *Chem Phys Impact,* 7 (2023) 100296.

40 Mzgin MA, Farouq EH, Design, Synthesis, Molecular Docking, Biological Evaluation, DFT and ADME Studies of novel bisquinazolinone derivatives. *Inorg Chem Commun,* 158 (2023) 111499.

41 Rajaraman D, Athishu AL, Nethaji P, Ravali V, One-pot synthesis, NMR, quantum chemical approach, molecular docking studies, drug-likeness and *in silico* ADMET prediction of novel 1-(2, 3 dihydrobenzo[b][1, 4]dioxin-6-yl)-2-(furan-2-yl)-4, 5-diphenyl- 1 H -imidazole derivatives. *J Mol Struct,* 1273 (2023) 134314.

42 Abduvakhid J, Utkirjon H, Hakim H, Noureddine I, Ahmad A, Intermolecular interactions in ethanol solution of OABA: Raman, FTIR, DFT, M062X, MEP, NBO, FMO, AIM, NCI, RDG analysis. *J Mol Liq,* 377 (2023) 121552.

43 Jeyavijayan S, Spectroscopic (FTIR, FT-Raman), molecular electrostatic potential, NBO and HOMO–LUMO analysis of P-bromobenzenesulfonyl chloride based on DFT calculations. *Spectrochim Acta A Mol Biomol Spectrosc,* 136 (2015) 890.

44 Ronald JG, Ronald JG, Paul LAP, Popelier PLA, Chemical Bonding and Molecular Geometry: *From Lewis to Electron Densities* (Oxford University Press, New Delhi) 2001, 268.

45 Ronald JG, Istvan H**,** *The VSEPR Model of Molecular Geometry* (dover publication. Inc. Mineola.New York) 2012, 236.